A hollow microcavity enzymatic fuel cell for in vivo energy harvesting

Anastasiia Berezovska, Paulo Henrique M. Buzzetti, Yannig Nedellec, Chantal Gondran, Fabien Giroud, Andrew J. Gross, Stephane Marinesco, Serge Cosnier

Cell Reports
Physical Science

CellPress
OPEN ACCESS

Article

A hollow microcavity enzymatic fuel cell for *in vivo* energy harvesting

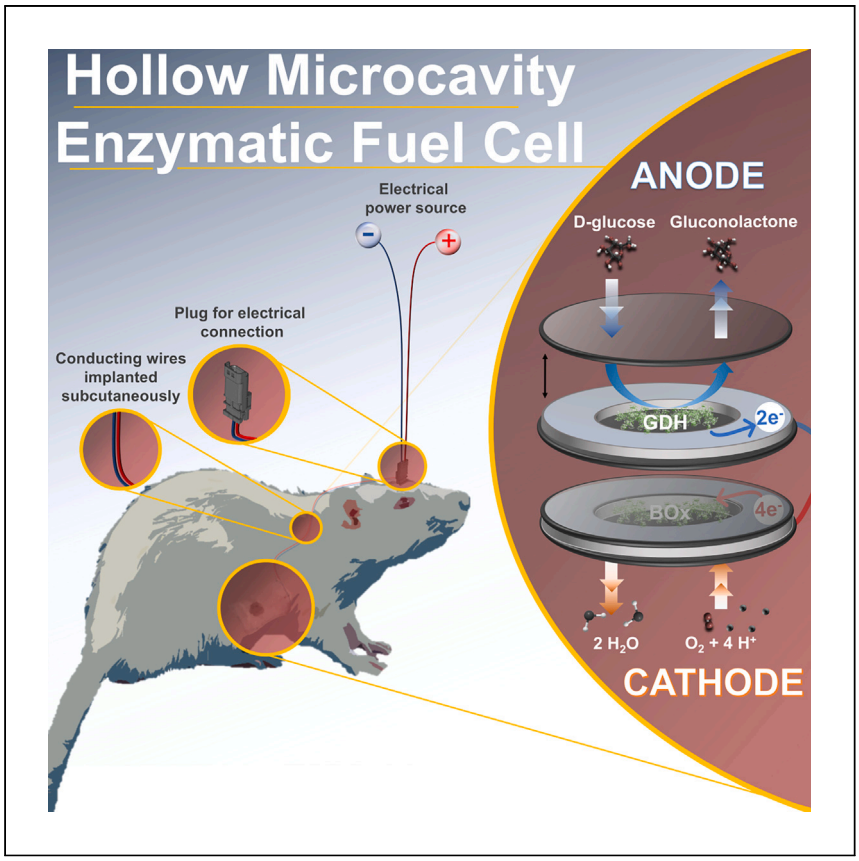

Berezovska et al. report a glucose/O_2 enzymatic fuel cell (EFC) using a "cavity electrode" design for biocatalyst entrapment. The new hollow EFC exhibits impressive performance and good stability. Implanted in living rats, voltages show a strong correlation with animal weight. Postmortem analysis confirms robustness and biocompatibility, offering a significant advancement in long-lasting implantable EFCs.

Anastasiia Berezovska, Paulo Henrique M. Buzzetti, Yannig Nedellec, ..., Andrew J. Gross, Stephane Marinesco, Serge Cosnier

serge.cosnier@univ-grenoble-alpes.fr

Highlights

"Hollow" bioanodes with FAD-glucose dehydrogenase show remarkable stability

In vivo implantation of a hollow glucose/O_2 enzymatic fuel cell beyond 70 days

Autopsy findings show no rejection signs, demonstrating effective biocompatibility

"Hollow" bioelectrodes exhibit electrocatalytic activity after 74-day implantation

Berezovska et al., Cell Reports Physical Science 5, 102203
September 18, 2024
Published by Elsevier Inc.
https://doi.org/10.1016/j.xcrp.2024.102203

Please cite this article in press as: Berezovska et al., A hollow microcavity enzymatic fuel cell for *in vivo* energy harvesting, Cell Reports Physical Science (2024), https://doi.org/10.1016/j.xcrp.2024.102203

Cell Reports
Physical Science

CellPress
OPEN ACCESS

Article

A hollow microcavity enzymatic fuel cell for *in vivo* energy harvesting

Anastasiia Berezovska,[2,4] Paulo Henrique M. Buzzetti,[2,4] Yannig Nedellec,[2] Chantal Gondran,[2] Fabien Giroud,[2] Andrew J. Gross,[2] Stephane Marinesco,[3] and Serge Cosnier[1,2,5,*]

SUMMARY

Enzymatic fuel cells (EFCs) have emerged in recent years as a promising power source for wearable and implantable electronic devices. Here, successful *in vivo* implantation of a glucose/O_2 EFC beyond 70 days is reported that exploits an innovative "cavity electrode" concept for biocatalyst entrapment to address lifetime and biocompatibility issues. The hollow bioanode shows long-term *in vitro* bioelectrocatalytic storage stability of >25 days. The hollow buckypaper-based EFC exhibits attractive maximum voltage and power outputs of 0.62 V and 0.79 mW cm^{-2}, respectively, and high storage stability of ~80% after 19 days. The maximum *in vivo* performance outputs are 0.34 ± 0.05 V and 38.7 ± 4.7 μW. After 74 days in Sprague-Dawley rats, the hollow EFC continues to present a stable 0.59 V. Postmortem analysis confirms high-level robustness and operational performance. Autopsy findings reveal no signs of rejection and demonstrate effective biocompatibility.

INTRODUCTION

Implantable electronic devices (IEDs), such as the cardiac pacemaker or drug delivery devices, have revolutionized the management and treatment of human health and diseases.[1] In recent years, a new era of implantable bioelectronics devices has emerged, ranging from electrochemical devices for therapeutic wound healing and deep brain stimulation to diagnostic devices such as continuous glucose sensors for diabetes management.[1–3] The development of IEDs is driven by a growing demand for personalized and precise medicine as well as advances in wireless communication and electronics device miniaturization, which include lowering the power and size requirements. IEDs require a dedicated portable energy source that can guarantee normal operation of periods of several months to years, depending on the target application. Miniature batteries are conventionally employed but are considered relatively bulky and require periodic replacement. Many miniaturized batteries are also dependent on limited natural resources and involve toxic battery chemicals. The need for periodic replacement is a burden, since it limits device use and imposes the need for multiple surgeries if extended use of the IED is required. The development of alternative implantable power sources, such as energy harvesting and wireless power transfer, including inductive coupling, is therefore a subject of increasing importance.

Enzymatic fuel cells (EFCs) have emerged in recent years as promising power sources for wearable and implantable electronic devices.[3,4] EFCs can harvest electrical energy from chemical energy via the oxidation of organic fuels, such as sugars and alcohols (at the anode), coupled with the reduction of an oxidant, typically oxygen (at

[1]Center for Organic and Nanohybrid Electronics, Silesian University of Technology, Konarskiego 22B, 44-100 Gliwice, Poland

[2]Département de Chimie Moléculaire, CNRS UMR-5250, Université Grenoble Alpes, 38000 Grenoble, France

[3]Lyon Neuroscience Research Center, CNRS UMR-5292, University of Lyon, 69675 Bron, France

[4]These authors contributed equally

[5]Lead contact

*Correspondence: serge.cosnier@univ-grenoble-alpes.fr

https://doi.org/10.1016/j.xcrp.2024.102203

Please cite this article in press as: Berezovska et al., A hollow microcavity enzymatic fuel cell for *in vivo* energy harvesting, Cell Reports Physical Science (2024), https://doi.org/10.1016/j.xcrp.2024.102203

the cathode). The anode and cathode exploit oxidoreductase enzymes as catalysts that provide highly specific and selective bioelectrocatalytic reactions under physiologically relevant conditions and, thus, the possibility for clean energy harvesting with limited side reactions. For over a decade, significant attention has been directed toward the development of glucose/O_2 EFCs as implantable power sources owing to the possibility of extracting reasonable voltages, typically around 0.5 V, and power outputs ranging from tens to hundreds of microwatts from single cells *in vivo* or in artificial physiological fluids.[4,5] The possibility to extract microwatt power outputs at practical voltages, as well as the ability to deliver power for more than a year, has been demonstrated under less challenging *ex vivo* conditions.[6,7] For example, EFC experiments are typically performed at elevated substrate/oxidant concentrations, in the presence of convection, at optimum pH, and, sometimes, in the presence of high buffer salt concentrations. The possibility to power electronic devices, such as sensors and stimulators, *in vivo* or in artificial fluids has been demonstrated.[8] Nevertheless, there are many challenges to overcome for EFC to emerge as a reliable power source; for example, the limited power output, lifetime, and biocompatibility of devices. Alternative bioelectrode-compatible sterilization protocols and further improvements in miniaturization are additional factors to take into account.

Recent advances in the field of *in vivo* EFCs include the development of biocompatible interfaces, such as zwitterionic[9] and chitosan[10] matrices, and our recent report on the ongoing development of bactericidal treatments for implanted enzymatic bioelectrodes and EFCs.[11] Lately, we started to explore the possibility of using enzymes and redox mediators in solution as opposed to their conventional immobilization at surfaces. For example, we developed the solubilized EFC concept as a strategy to help overcome EFC lifetime limitations. With the presence of freely diffusing enzymes, mediators, and substrates, we showed a power loss of only ~26% after 7 days of continuous charge-discharge cycling at 50 μA, which corresponded to very promising performance for quasi-continuous power operation.[12] The use of freely diffusing enzymes and mediators is considered attractive for bioelectrocatalysis; for example, thanks to orientation and improved mass transfer effects. More recently, we reported an original "hollow" or "cavity" bioelectrode concept fabricated with carbon nanotube (CNT) materials.[13] In this first design, we developed a Bilirubin oxidase (BOx)-based biocathode that was constructed using two opposed and spatially separated carbon buckypapers (BPs) with a microcavity between them for storage of enzyme initially present in powder form. Thanks to the bioelectrocatalyst entrapment inside the cavity, the optimized hollow microcavity biocathode retained good electroactivity (i.e., 30% of its initial activity after 3 months and 11% after 6 months of periodic testing) and was still capable of delivering ~120 μA cm^{-2}. The microcavity bioelectrodes benefit from the use of lab-made and commercial BPs that have been proven to have a very high surface area and flexible materials for bioelectrode construction.[14,15]

Lab-made BP electrodes, to the best of our knowledge, have not yet been reported for use in *in vivo* EFCs despite their attractive properties, including their thin form factors (~200–300 μm thick), which make them perfectly suitable for hollow-electrode experiments. In the present work, we report the development of a hollow-electrode enzymatic biofuel cell that builds on the concept of enzyme entrapment in solution at high-surface-area BP electrodes (Figure 1A). A BOx-powder-based biocathode and an optimized FAD-GDH powder-based bioanode are used for the EFC elaboration. Electrochemical, bioelectrocatalytic, and EFC performance are first examined *in vitro* before moving on to device implantation and long-term *in vivo*

Please cite this article in press as: Berezovska et al., A hollow microcavity enzymatic fuel cell for *in vivo* energy harvesting, Cell Reports Physical Science (2024), https://doi.org/10.1016/j.xcrp.2024.102203

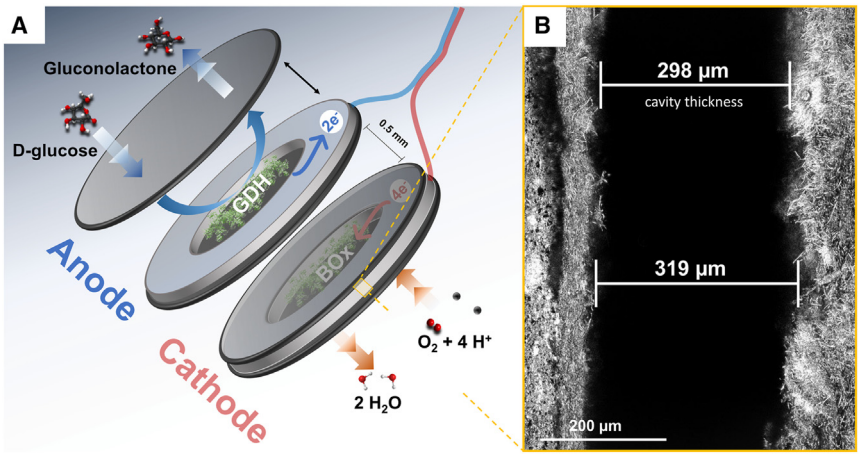

Figure 1. Hollow enzymatic electrodes
(A) Top-down and side view.
(B) Laser image of the vertical cross-section of the hollow biocathode. Scale bar, 200 µm.

performance testing. Postmortem studies, including voltammetric half-cell characterization, are also reported.

RESULTS AND DISCUSSION

Miniaturization of hollow BOx bioelectrodes for bioelectrocatalytic reduction of oxygen

With a view to developing the first hollow EFC and its application *in vivo*, our first objective was to miniaturize the hollow bioelectrodes and to test their performance in more physiologically relevant conditions; i.e., at pH 7.4. The electrode outer diameter was decreased from 30 mm to 13 mm, providing a more practical and reasonable implantable device footprint. A laser image of the vertical cross-section of a hollow electrode is given in Figure 1B, showing a cavity volume of 12.0 ± 1 µL for a hollow biocathode composed of a lab-made BP modified with hemin via a one-pot method ($L_{H(OP)}$), coupled with an unmodified commercial BP (C_u). The hollow biocathode conception involved a direct electron transfer (DET) mechanism reported previously, since it exhibited attractive long-term stability.[13,14] In this design, lab-made BPs were functionalized with hemin molecules (an analog of the enzyme's natural substrate, bilirubin) through physical interactions (e.g., π-π stacking on CNT sidewalls) to promote oriented immobilization of BOx by electrostatic interactions. This orientation is crucial for achieving efficient electron transfer.[16–19]

The cyclic voltammograms recorded in Ar-, air-, and O_2-saturated solutions are shown in Figure 2A. First electrochemical testing displayed high onset potentials of ~0.56 V at pH 7.4 for the oxygen reduction reaction, which is consistent with our previous studies with efficient enzyme orientation of BOx. As expected, the electrocatalytic currents strongly depend on the oxygen concentration. In quiescent air-saturated solution, the current reaches −0.20 mA at 0.405 V before dropping due to diffusion limitations. Meanwhile, in the presence of oxygen-saturated solution, the catalytic current increases to −0.86 mA (−1.12 ± 0.18 mA cm^{-2}, 0.77 cm^2) at 0.3 V before reaching a semi-plateau associated with diffusion limitations owing to the finite diffusion layer thickness. Since a DET mechanism is involved here, it is important to note that the recorded electrocatalytic currents included a contribution from the unmodified commercial BP forming the cavity electrode. According to our previous work on commercial and cavity BPs, this current accounts for a maximum of

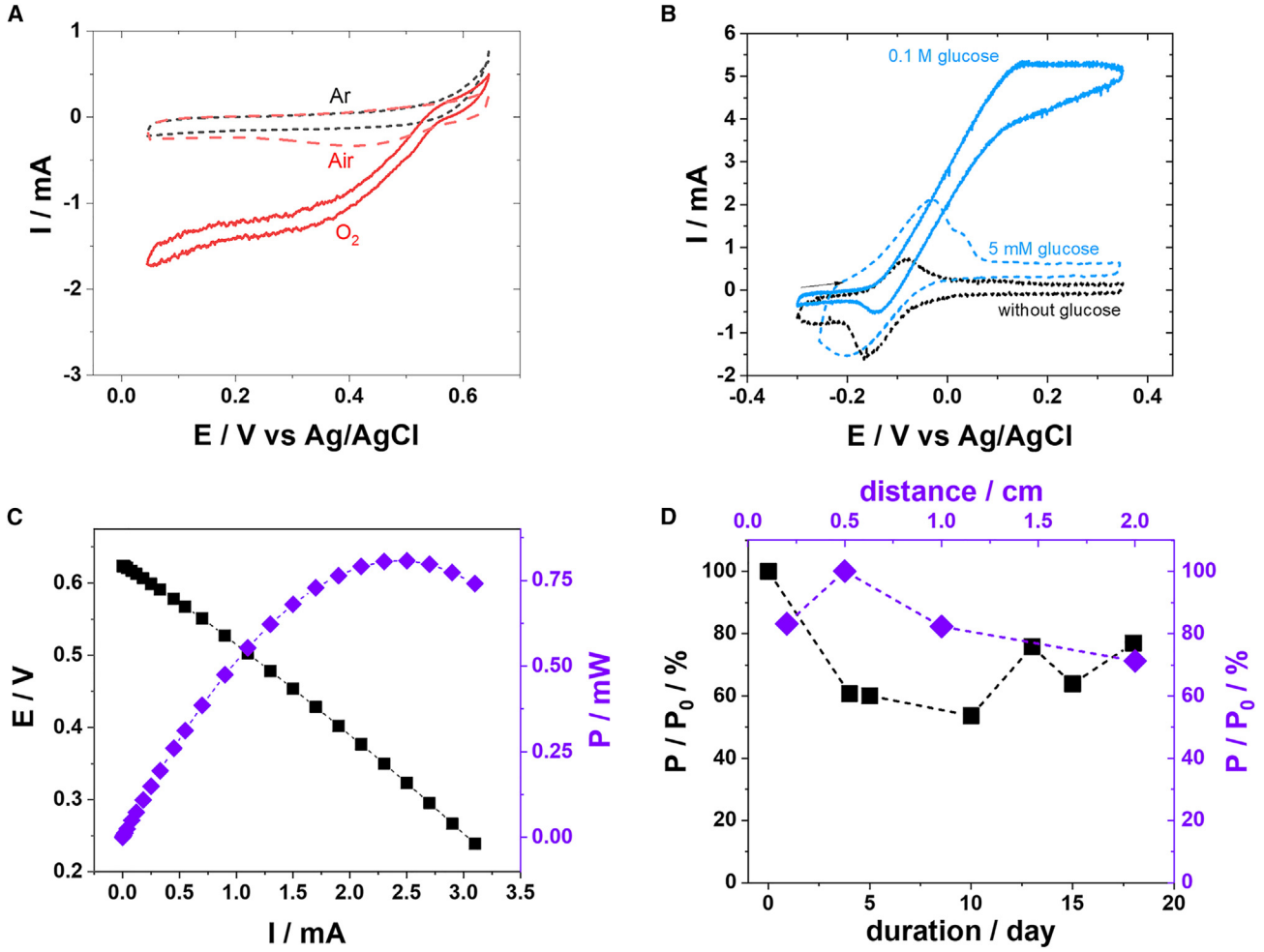

Figure 2. Electrocatalytic studies of the hollow half-cells and *in vitro* hollow EFC power outputs as functions of time and distance between half-cells

(A) CVs recorded in 0.1 M PB (pH 7.4) at 1 mV s^{-1} under Ar-saturated (dots), air-saturated (red dashes), and O_2-saturated conditions (red line) at hollow $C_uL_{H(OP)}$-based biocathodes.

(B) CVs recorded in 0.1 M PB (pH 7.4) under Ar at 1 mV s^{-1} in the absence (dots), in the presence of 0.1 M glucose (blue line), and in the presence of 5 mM glucose (blue dashes) at hollow $CL_{PLQ(DC)}$-based bioanodes.

(C) Hollow EFC polarization (■) and power curves (◆) recorded in 0.1 M PB (pH 7.4) with 0.1 M glucose under O_2-saturated conditions via galvanostatic discharge with applied currents ranging from 0.005–3.100 mA for 10 s.

(D) Evolution of the hollow EFC power as a function of inter half-cell distance via potentiostatic discharge at 0.5 V for 10 s (■) and EFC power (inter half-cell distance of 0.5 cm) as a function of duration via potentiodynamic polarization at 0.2 mV s^{-1} (◆).

10%–12% of the current recorded at the biocathodes.[13,20] The catalytic current is smaller than the −1.63 mA (−2.11 mA cm^{-2}) at 0.3 V observed at pH 6.5 (Figure S2). This drop is consistent with the activity loss of BOx beyond neutral pH, which is due to the structural dependence of the T1 copper center on protonation/deprotonation of its amino acid residue neighborhoods.[18] At the same pH and potential, the catalytic current reported here for the smaller cavity design was in the same range as that obtained for larger electrodes (approximately −1.16 mA cm^{-2}, S = 2.26 cm^2).

"One-pot" and "drop coat" quinone-functionalized BPs for bioelectrocatalytic oxidation of glucose

We then developed the first hollow enzymatic bioanodes with FAD-GDH (FAD-glucose dehydrogenase) as a favorable alternative to glucose oxidase in terms of specificity, activity, and stability.[21] As this enzyme does not display a DET

Please cite this article in press as: Berezovska et al., A hollow microcavity enzymatic fuel cell for *in vivo* energy harvesting, Cell Reports Physical Science (2024), https://doi.org/10.1016/j.xcrp.2024.102203

mechanism, conventional quinone mediators (1,4-naphthoquinone [NQ]and 1,10-phenanthroline-5,6-dione [PLQ]) were used to ensure the protein "wiring" for glucose oxidation via mediated electron transfer (MET) at low potentials.[14] Two configurations of hollow electrodes were compared: one based on BP whose nanotubes were modified by redox mediators before the BP fabrication (one pot) and the other based on BP modified after their elaboration (drop coat). Table S1 summarizes the composition of both the electrodes and the hollow bioelectrodes used in this work.

Voltammograms recorded in argon exhibited well-defined electrochemical processes at $E_{1/2,NQ} = -185 \pm 10$ mV and $E_{1/2,PLQ} = -130 \pm 10$ mV, consistent with surface-bound species that are accessible to the electrolyte (Figure S3). "One-pot" electrodes displayed slightly faster electron transfer than "drop coat" electrodes, as shown by the smaller ΔE_p for each quinone ($C_uL_{NQ(OP)}$ = 30 mV vs. $CL_{NQ(DC)}$ = 97 mV and $C_uL_{PLQ(OP)}$ = 65 mV vs. $CL_{PLQ(DC)}$ = 82 mV). This could be explained by the large surface coverage obtained after functionalization. The values were estimated to be $\Gamma_{NQ(OP)} = 3.84\ 10^{-8}$ mol cm^{-2}, $\Gamma_{PLQ(OP)} = 1.26\ 10^{-7}$ mol cm^{-2}, $\Gamma_{NQ(DC)} = 6.55\ 10^{-7}$ mol cm^{-2} and $\Gamma_{PLQ(DC)} = 7.18\ 10^{-7}$ mol cm^{-2} (which represent a 16.9- and 5.6-fold increase, respectively). However, the low surface coverage of NQ suggests that this quinone is prone to being washed away during the one-pot fabrication. Conversely, drop coating afforded reproducible functionalized electrodes and allowed for the functionalization of the commercial BP support so that the complete inner geometric surface exposed to solubilized enzyme can participate in MET.

Next, bioelectrocatalytic studies for the glucose oxidation reaction were conducted for all four different types of hollow bioanodes with the same enzyme loading (4 mg) and cavity size. The significance of having a high mediator loading is clearly highlighted by the better efficiency of PLQ as a mediator for FAD-GDH in terms of catalytic current output (turnover) compared to the NQ at electrodes with very similar surface coverage (Figure S3). In the presence of 0.1 M glucose, CV (cyclic voltammogram) showed sigmoidal current shapes that corresponded to a well-defined bioelectrocatalytic signal that reached a nearly steady state at higher potentials. In agreement with the calculated $E_{1/2}$ values, the onset potential for glucose oxidation was lower for NQ compared to PLQ, approximately −0.21 V and −0.14 V, respectively. For one-pot hollow bioanodes, the maximum bioelectrocatalytic currents at 0.3 V reached 0.46 mA (1.20 mA cm^{-2}, S = 0.385 cm^2) with NQ and 2.88 mA (7.48 mA cm^{-2}, S = 0.385 cm^2) when PLQ was used. For drop coat bioanodes, the CVs exhibited similar shapes as observed for the one-pot hollow BP with maximal current reached near 0.1 V for both quinones. The $CL_{NQ(DC)}$ hollow bioanode exhibited a catalytic maximum current of 4.06 mA (5.27 mA cm^{-2}, S = 0.77 cm^2), representing a 9-fold improvement compared to the $C_uL_{NQ(OP)}$ bioanode. At the $CL_{PLQ(DC)}$ bioanode, a catalytic current of 5.27 mA (6.84 mA cm^{-2}; S = 0.77 cm^2) was reached that represents a 2-fold improvement (Figure 2B). We finally evaluated the electrocatalytic behavior at a low glucose concentration for the best-performing hollow bioanodes. At physiologically relevant conditions (i.e., 5 mM glucose), the bioanodes were able to generate between 0.48 and 0.55 mA (0.62–0.71 mA cm^{-2}) in the range of 0.1 V–0.35 V.

The long-term storage stability was evaluated by periodically recording catalytic CVs in fresh PB buffer in the presence of 0.1 M glucose (Figure S4). For this step, electrode configurations were investigated ($CL_{NQ(DC)}$, $C_uL_{PLQ(OP)}$, and $CL_{PLQ(DC)}$) due to their ability to sustain the most attractive catalytic currents on day 0. After 20–26 days with 6 tests performed for each electrode type, the drop-coat hollow

Please cite this article in press as: Berezovska et al., A hollow microcavity enzymatic fuel cell for *in vivo* energy harvesting, Cell Reports Physical Science (2024), https://doi.org/10.1016/j.xcrp.2024.102203

bioanodes still exhibited ~1–1.4 mA (~1.30–1.82 mA cm^{-2}), while less than 0.1 mA (0.26 mA cm^{-2}) was obtained at the one-pot hollow bioanode after only 17 days. The different time-dependent behaviors were not evaluated further, but evidence for a catalytic "burst" effect was observed at day 5 to day 7 for $CL_{PLQ(DC)}$, which is highly unusual and could be linked to the delayed solubilization of the enzyme and/or mediator in the cavity that results in an increased amount of electrical wiring. The phenomena may be also ascribed to the hydrophobic and heterogeneous nature of the BP. Moreover, the storage stability outperforms what we reported previously using an optimized single one-pot BP bioanode based on PLQ and FAD-GDH, where the current density dropped from almost 6 mA cm^{-2} to ~1 mA cm^{-2} after only 10 days.[14]

Glucose/O_2 *in vitro* hollow EFC

After confirming the bioelectrocatalytic performance of the half-cells, a hollow-electrode based EFC was mounted with the $C_uL_{H(OP)}$ biocathodes and the optimized $CL_{PLQ(DC)}$ bioanodes. The two electrodes were placed face to face in PB containing 0.1 M glucose and O_2-saturated (≈ 1.1 mM). The tests with saturating substrate concentrations were chosen to identify the maximum voltage and power output that may be reached by the device. A large OCV (open circuit potential) of 0.62 V was observed that agrees with the estimated maximum voltage of 0.66 V from the half-cell measurements. The OCV is notably higher than the 0.50 V obtained previously in similar conditions for a dialysis bag biofuel cell prepared with CNT biopellets.[11] Galvanostatic discharges were performed with currents ranging from 0.005 to 3.100 mA and an operation time of 10 s to determine the polarization (Figure S5) and power curves (Figure 2C). The shape of the polarization curves obtained during 10 s indicates that the hollow EFCs do not exhibit excessive capacitive discharge contributions after the first 2 s of operation. The hollow EFC produced a maximum average power output of 0.61 ± 0.05 mW (0.79 ± 0.07 mW cm^{-2}, S = 0.77 cm^2), which compares to the ~0.1 mW obtained with biopellet EFCs tested under the same conditions.[11]

In a side experiment, we investigated the influence of the inter-electrode spacing (0.2–2.0 cm) between the two bioelectrodes. For these measurements, the power was determined from the current obtained by potentiostatic discharge at 0.50 V for 10 s (Figure 2D). These results point to a near optimal spacing of around 0.5 cm. A shorter distance (x = 0.25 cm) led to an approximately −20% decrease, while a spacing greater than $x \geq 1.0$ cm resulted in a small but progressive decrease down to −25% for the largest inter-electrode spacing. The results are not surprising, considering that very closely spaced electrodes can hinder substrate diffusion while large inter-electrode spacing can amplify ohmic losses.[22] Finally, we evaluated the storage stability of the EFC with 0.5-cm electrode spacing in terms of the power output obtained on different days relative to the initial power output, P_0. Figure 2D shows the storage stability, revealing excellent storage stability and activity after 19 days with ~70% of the initial P_0 remaining. This progressive decay is attributed to the loss of activity of the biocathode that limits the overall power performance of the EFC. The increase in stability performance beyond 1 week is very unusual for an *in vitro* EFC and points to a "catalytic boost" effect linked to biocatalyst storage and solubilization effects thanks to the cavity design.

In vivo glucose/O_2 hollow EFC in a dialysis bag with surgical tissue

After demonstrating attractive *in vitro* performance under largely ideal conditions, implantation experiments were carried out in two adult Sprague-Dawley rats, referred to here as SDR1 and SDR2. For the *in vivo* EFCs, the protocols were adjusted

Please cite this article in press as: Berezovska et al., A hollow microcavity enzymatic fuel cell for *in vivo* energy harvesting, Cell Reports Physical Science (2024), https://doi.org/10.1016/j.xcrp.2024.102203

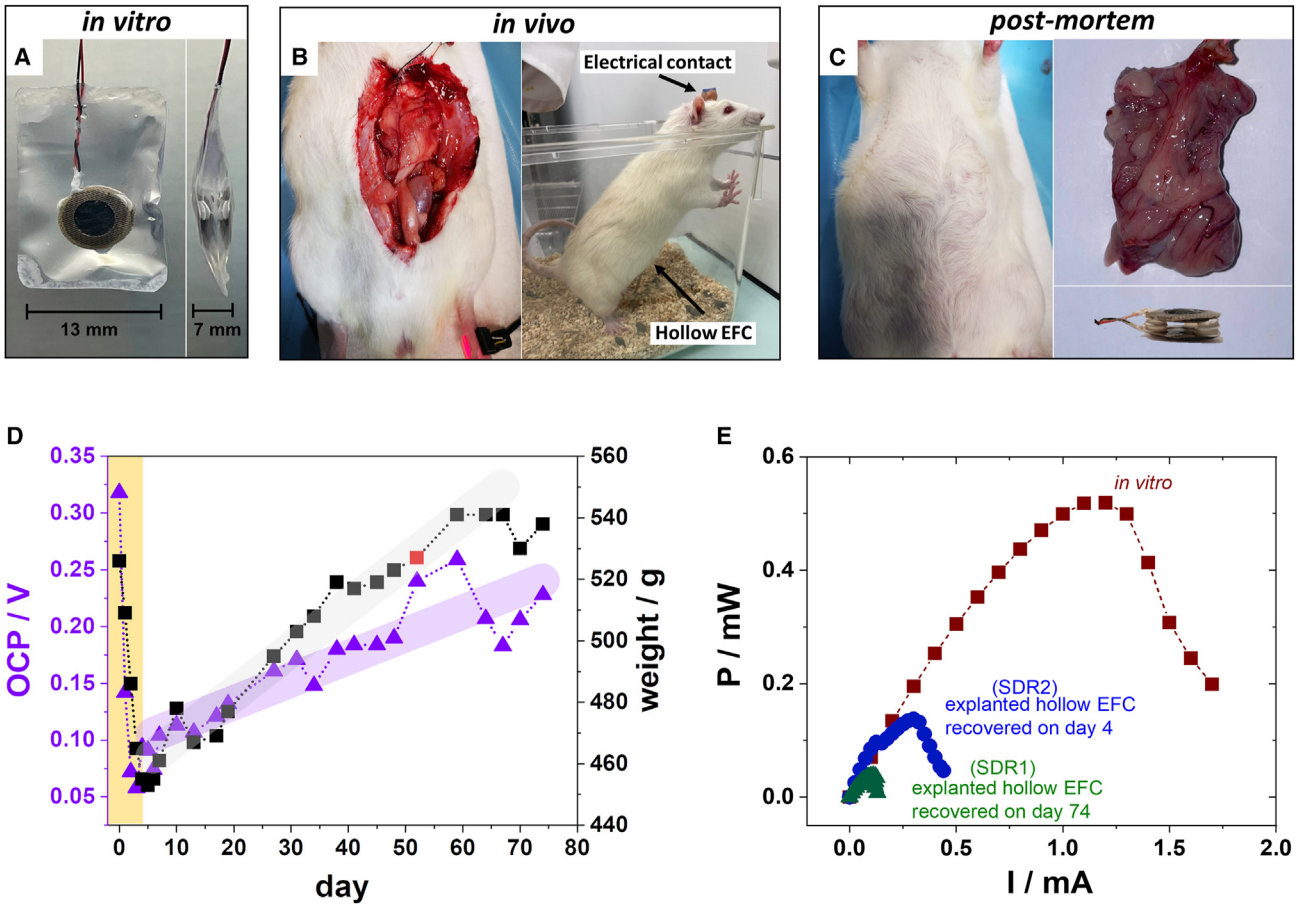

Figure 3. Pictures of the final hollow EFC *ex situ* and of the rat with the implanted EFC and the corresponding power performance of the hollow EFCs

(A) Face and side profile photographs of the hollow EFC inside a sealed dialysis bag.

(B) Photographs taken during and after EFC implantation surgery of the rat that display the location of the implanted EFC and the electrical contact.

(C) Photograph of the rat's abdominal implanted region (74th day of implantation) and the hollow EFC recovered after euthanasia within the adipose tissues (above) and *ex situ* outside of the sealed bags (below).

(D) Evolution of the weight (■) and the OCV (▲) of the rat with the implanted hollow EFC as a function of time.

(E) Estimated power profiles for the *in vitro* EFC (■) and the postmortem-explanted hollow EFC recovered on day 4 (●) and day 76 (▲) analyzed *in vitro* (power profiles were calculated from forward scans of anodic and cathodic CV curves given in Figure S7).

slightly to enhance sterility and biocompatibility. We utilized a dialysis bag wrapped with a biocompatible porous mesh specifically designed for surgical applications. Figure 3A displays photographs of the face and side profiles of the hollow EFC device within the dialysis bag. For surgery, in brief, SDR1 and SDR2 (~530 g) were anesthetized with isoflurane and subjected to two incisions through the skull (5 mm long) and the abdominal wall (6–7 cm long). A surgical mesh-coated hollow EFC device was then carefully placed on the viscera, and the abdominal wall and the skin were sutured (complete details can be found in the supplemental information). Figure 3B depicts the location where a hollow EFC device was implanted, along with a post-surgery photograph of the rat.

Just before implantation under *in vitro* non-saturated O_2 conditions and with 5 mM glucose, the hollow EFCs presented an OCV of 0.49 ± 0.13 V. Just after the rats had recovered from the anesthesia used during the implantation, the hollow EFCs exhibited an OCV of 0.34 ± 0.05 V. Potentiostatic discharge at 75% of the OCV values for 10 s revealed a maximum power output of 38.7 ± 4.7 μW (50.3 ± 6.1 μW cm^{-2},

S = 0.77 cm^2). Although the voltage values were much lower than those observed under more ideal saturated substrate conditions, they were higher or similar to the OCV values reported previously for implanted biopellet EFCs.[11,23,24] The power output was also higher when compared with data provided in the aforementioned literature; i.e., power outputs ranging from 2–10.4 μW. The OCV values as well as the animal's weight were monitored periodically. Figure 3D displays a swift drop in OCV during the initial days following implantation, which is a common observation for *in vivo* EFCs. On the fourth day, both the OCV and the rat's weight reached their most critical values of 74 ± 10 mV and approximately 450 g, respectively. Consequently, a low power output value of 0.5 ± 0.1 μW was observed. The large OCV drop is strongly correlated with the weight of the animal in this study. Since food intake was severely reduced during the first days after surgery, it is possible that low glycemia could at least in part explain this drop in OCV, highlighting the influence of the health state of the animal on performance in the early stages after implantation. For example, metabolic effects (i.e., more limited substrate concentrations available) and/or inflammatory reaction effects could hinder O_2 mass transport due to poorly vascularized connective tissue around the implant and can also result in the release of deactivating substrates.[25] Due to the aforementioned factors, SDR2 had to be euthanized on day 4, whereas SDR1 could be monitored for 74 days. Starting from day 5, SDR1 experienced a gradual weight increase of approximately 1.5 g day^{-1} that is consistent with effective recovery of the rat. This was accompanied by an OCV elevation of 2.0 ± 0.2 mV day^{-1}, showing a steady improvement in EFC performance as well as health over time. The operational OCV beyond 1 month ranged from 0.17–0.26 V, with the maximum operational OCV observed at around 2 months, and was still below the OCV measured after implantation (0.318 V).

This time frame also corresponds to the point when the rat made an apparent full recovery with good weight stability (527 ± 6 g) between days 60 and 74. On day 74, the last *in vivo* OCV measurement (0.23 V) was recorded before the rat was euthanized. After 2.5 months, it was decided to euthanize the rat according to the regulations imposed by the ethics committee.

Postmortem analysis of SDR1 revealed complete skin recovery after 74 days of implantation (Figure 3C). Autopsy findings showed no signs of rejection or inflammation in the visceral region where the device was implanted. The EFC device was entirely enveloped by a thick layer of vascularized tissue (Figure 3C), which is consistent with a healthy immune response and effective biocompatibility. Histological analysis revealed that the adipose tissue was fully fused to both the artificial mesh and the dialysis bag, as shown in Figure S6. Subsequently, the recovered hollow EFC, after removal of the bags and adipose tissue, was immersed in 0.1 M PB (pH 7.4) containing 0.1 M glucose and O_2 saturation. The OCV initially increased to 0.42 V and then reached a maximum value of 0.59 V 48 h post autopsy. This almost full recovery in OCV (−6%) suggests that the hollow EFC exhibited a high level of robustness and remained operational even after 74 days *in vivo*.

In a concluding supplemental experiment, both hollow half-cells that were explanted from SDR1 and SDR2 were examined under saturated substrate concentrations to provide further insights into the EFCs' performance and limiting electrodes. The data reveal well-defined bioelectrocatalytic curves for both bioanodes and biocathodes (Figure S7). Estimated power profiles were calculated from first sweeps of CV experiments (similar to linear sweep voltammetry) to assess power loss over an extended period. Initially, a hollow EFC could generate up to 608 ± 56 μW (790 ± 73 μW cm^{-2}) in

Please cite this article in press as: Berezovska et al., A hollow microcavity enzymatic fuel cell for *in vivo* energy harvesting, Cell Reports Physical Science (2024), https://doi.org/10.1016/j.xcrp.2024.102203

Table 1. Enzymatic hollow half-cell bioelectrocatalytic performance recovered *in vivo* and tested *in vitro* under substrate-saturated conditions

	Days implanted	Half-cell analysis	Bioanode (mA cm^{-2})[a]	Biocathode (mA cm^{-2})[b]	Power output (μW cm^{-2})
In vitro	–	–	6.06 ± 0.78	−1.12 ± 0.18	790 ± 73
SDR2	4	4^{th} day	3.20 (−53%)	−0.43 (−62%)	180
SDR1	74	76^{th} day	0.15 (−98%)	−0.29 (−74%)	49

SDR1, Sprague-Dawley rat 1; SDR2, Sprague-Dawley rat 2.
[a]Current density measured from CV experiments recorded at 1 mV s^{-1} at 0.3 V in the presence of 0.1 M glucose.
[b]Current density measured from CV experiments recorded at 1 mV s^{-1} at 0.3 V in the presence of O_2 saturation.

saturation conditions. At days 30 and 76, the maximal power output dropped to 138 μW (180 μW cm^{-2}) and 38 μW (49 μW cm^{-2}), respectively (Figure 3E). Table 1 compiles the evolution of *in vivo* recovered hollow half-cell bioelectrocatalytic performance *in vitro* under substrate saturation conditions.

In summary, despite the exciting prospects offered by biofluids for *in vivo* electrical energy generation to power battery-less implanted electronic devices, significant hurdles related to power output, lifetime, and biocompatibility remain, delaying their practical applications. In this work, mainly addressing lifetime and biocompatibility issues, we present the *in vivo* implantation of a glucose/O_2 EFC based on an innovative concept of biocatalyst entrapment using carbon BPs. A hollow bioanode involving a drop-coated quinone for a MET mechanism with FAD-GDH during catalytic glucose oxidation was reported. It presented *in vitro* long-term storage stability greater than 25 days. The bioelectrocatalytic performance of the hollow enzymatic half-cells was evaluated before complete EFC characterization. A glucose/O_2 hollow EFC displayed attractive 0.62 V maximum voltage and 0.79 ± 0.07 mW cm^{-2} maximum power output. Moreover, an unusual behavior linked to enzyme storage and solubilization provides notable storage stability and activity (>80% vs. initial power output) over 19 days. Implanted into the abdomen of adult Sprague-Dawley rats, the glucose/O_2 hollow EFC initially displayed OCV of 0.34 ± 0.05 V and power output of 38.7 ± 4.7 μW, followed by a progressive loss attributed to the animal's immune response. The OCV was monitored until the animal's health state and weight recovered over 74 days. Autopsy findings showed no sign of rejection or inflammation, and vascularized tissue enveloping the EFC demonstrated effective biocompatibility. *In vitro* postmortem analysis revealed that the hollow half-cell structure remained intact and still presented a well-defined bioelectrocatalytic response.

EXPERIMENTAL PROCEDURES

Materials and methods

A complete description of the materials and methods used in this study (supplemental experimental procedures), along with the results that directly support the main conclusions, can be found in the supplemental information.

RESOURCE AVAILABILITY

Lead contact

Requests for further information and resources should be directed to and will be fulfilled by the lead contact, Serge Cosnier (serge.cosnier@univ-grenoble-alpes.fr).

Materials availability

This study did not generate new unique reagents.

CellPress OPEN ACCESS

Cell Reports Physical Science Article

Data and code availability

This study did not generate any datasets.

ACKNOWLEDGMENTS

The authors gratefully acknowledge support from the platform Chimie NanoBio ICMG FR 2607 (PCN-ICMG) and financial support from the French National Research Agency (Agence Nationale de la Recherche [ANR]) under references ANR-18-CE09-0022 and ANR-20-CE05-0006-01, LabEx ARCANE (ANR-11-LABX-0003-01), and CBH-EUR-GS ANR-17-EURE-0003). The authors acknowledge financial support from the Région Auvergne-Rhône-Alpes 1801164901-41024 Program FLEXCELL. We are grateful to the Lyon Neuroscience Research Center animal facility, Mr. Gianni Raponi for daily animal care, and to Dr. Vet. Manon Dirheimer for veterinary advice on animal welfare. Annabelle Bouchardon and the CIQLE technological platform performed histological analyses of the conjunctive tissue around the hollow EFC.

AUTHOR CONTRIBUTIONS

The manuscript was written with contributions from all authors. Conceptualization, A.B., P.H.M.B., Y.N., S.M., and S.C.; methodology, A.B., P.H.M.B., Y.N., C.G., F.G., A.J.G., S.M., and S.C.; formal analysis, A.B., P.H.M.B., Y.N., F.G., A.J.G., and S.M.; investigation, A.B., P.H.M.B., Y.N., C.G., F.G., S.M., and S.C.; data curation, A.B., P.H.M.B., Y.N., F.G., and S.M.; validation, A.B., P.H.M.B., Y.N., F.G., A.J.G., S.M., and S.C.; writing – original draft, A.B., P.H.M.B., C.G., F.G., A.J.G., S.M., and S.C.; writing – review and editing, A.B., P.H.M.B., F.G., A.J.G., and S.C.; supervision, S.M. and S.C.; funding acquisition, S.M. and S.C. All authors have given approval to the final version of the manuscript.

DECLARATION OF INTERESTS

A.B., P.H.M.B., Y.N., and S.C. hold a patent registration as inventors related to the technology described in this paper. The patent is registered under the following reference(s): International application number: PCT/EP2022/078570; Title: Enzyme Electrode Having an Integrated Reservoir; Applicants: Centre National de la Recherche Scientifique, Université Grenoble Alpes.

SUPPLEMENTAL INFORMATION

Supplemental information can be found online at https://doi.org/10.1016/j.xcrp.2024.102203.

Received: May 1, 2024
Revised: July 19, 2024
Accepted: August 20, 2024
Published: September 10, 2024

REFERENCES

1. Dinis, H., and Mendes, P.M. (2021). A comprehensive review of powering methods used in state-of-the-art miniaturized implantable electronic devices. Biosens. Bioelectron. *172*, 112781. https://doi.org/10.1016/j.bios.2020.112781.

2. Long, Y., Li, J., Yang, F., Wang, J., and Wang, X. (2021). Wearable and Implantable Electroceuticals for Therapeutic Electrostimulations. Adv. Sci. *8*, 2004023. https://doi.org/10.1002/advs.202004023.

3. Oppel, E., Kamann, S., Heinemann, L., Reichl, F.-X., and Högg, C. (2020). The implanted glucose monitoring system Eversense: An alternative for diabetes patients with isobornyl acrylate allergy. Contact Dermatitis *82*, 101–104. https://doi.org/10.1111/cod.13392.

4. Garland, N.T., Kaveti, R., and Bandodkar, A.J. (2023). Biofluid-Activated Biofuel Cells, Batteries, and Supercapacitors: A Comprehensive Review. Adv. Mater. *35*, 2303197. https://doi.org/10.1002/adma.202303197.

5. ul Haque, S., Nasar, A., Duteanu, N., and Pandey, S.; Inamuddin (2023). Carbon based-nanomaterials used in biofuel cells – A review. Fuel *331*, 125634. https://doi.org/10.1016/j.fuel.2022.125634.

6. Reuillard, B., Abreu, C., Lalaoui, N., Le Goff, A., Holzinger, M., Ondel, O., Buret, F., and Cosnier, S. (2015). One-year stability for a glucose/oxygen biofuel cell combined with pH reactivation of the laccase/carbon nanotube biocathode. Bioelectrochemistry *106*, 73–76. https://doi.org/10.1016/j.bioelechem.2015.04.009.

7. Karim, N.A., and Yang, H. (2021). Mini-Review: Recent Technologies of Electrode and System in the Enzymatic Biofuel Cell (EBFC). Appl. Sci. *11*, 5197. https://doi.org/10.3390/app11115197.

8. Huang, W., Zulkifli, M.Y.B., Chai, M., Lin, R., Wang, J., Chen, Y., Chen, V., and Hou, J. (2023). Recent advances in enzymatic biofuel cells enabled by innovative materials and techniques. Exploration *3*, 20220145. https://doi.org/10.1002/EXP.20220145.

9. Guo, Y., Chen, C., Feng, J., Wang, L., Wang, J., Tang, C., Sun, X., and Peng, H. (2022). An Anti-Biofouling Flexible Fiber Biofuel Cell Working in the Brain. Small Methods *6*, 2200142. https://doi.org/10.1002/smtd.202200142.

10. El Ichi-Ribault, S., Alcaraz, J.-P., Boucher, F., Boutaud, B., Dalmolin, R., Boutonnat, J., Cinquin, P., Zebda, A., and Martin, D.K. (2018). Remote wireless control of an enzymatic biofuel cell implanted in a rabbit for 2 months. Electrochim. Acta *269*, 360–366. https://doi.org/10.1016/j.electacta.2018.02.156.

11. Berezovska, A., Meiller, A., Marinesco, S., Nedellec, Y., Giroud, F., Gross, A.J., and Cosnier, S. (2023). Chlorhexidine digluconate exerts bactericidal activity vs Gram positive Staphylococci with bioelectrocatalytic compatibility: High level disinfection for implantable biofuel cells. Bioelectrochemistry *152*, 108435. https://doi.org/10.1016/j.bioelechem.2023.108435.

12. Hammond, J.L., Gross, A.J., Giroud, F., Travelet, C., Borsali, R., and Cosnier, S. (2019). Solubilized Enzymatic Fuel Cell (SEFC) for Quasi-Continuous Operation Exploiting Carbohydrate Block Copolymer Glyconanoparticle Mediators. ACS Energy

Lett. *4*, 142–148. https://doi.org/10.1021/acsenergylett.8b01972.

13. Buzzetti, P.H.M., Berezovska, A., Nedellec, Y., and Cosnier, S. (2022). Hollow Bioelectrodes Based on Buckypaper Assembly. Application to the Electroenzymatic Reduction of O2. Nanomaterials *12*, 2399. https://doi.org/10.3390/nano12142399.

14. Gross, A.J., Chen, X., Giroud, F., Abreu, C., Le Goff, A., Holzinger, M., and Cosnier, S. (2017). A High Power Buckypaper Biofuel Cell: Exploiting 1,10-Phenanthroline-5,6-dione with FAD-Dependent Dehydrogenase for Catalytically-Powerful Glucose Oxidation. ACS Catal. *7*, 4408–4416. https://doi.org/10.1021/acscatal.7b00738.

15. Gross, A.J., Holzinger, M., and Cosnier, S. (2018). Buckypaper bioelectrodes: emerging materials for implantable and wearable biofuel cells. Energy Environ. Sci. *11*, 1670–1687. https://doi.org/10.1039/C8EE00330K.

16. Göbel, G., and Lisdat, F. (2008). Organic interlayers for oxygen reducing electrodes based on bilirubin oxidase and MWCNT modified gold. Electrochem. Commun. *10*, 1691–1694. https://doi.org/10.1016/j.elecom.2008.08.049.

17. Lopez, R.J., Babanova, S., Ulyanova, Y., Singhal, S., and Atanassov, P. (2014). Improved Interfacial Electron Transfer in Modified Bilirubin Oxidase Biocathodes. Chemelectrochem *1*, 241–248. https://doi.org/10.1002/celc.201300085.

18. Lalaoui, N., Le Goff, A., Holzinger, M., and Cosnier, S. (2015). Fully Oriented Bilirubin Oxidase on Porphyrin-Functionalized Carbon Nanotube Electrodes for Electrocatalytic Oxygen Reduction. Chem. Eur J. *21*, 16868–16873. https://doi.org/10.1002/chem.201502377.

19. Xia, H.q., Kitazumi, Y., Shirai, O., and Kano, K. (2016). Enhanced direct electron transfer-type bioelectrocatalysis of bilirubin oxidase on negatively charged aromatic compound-modified carbon electrode. J. Electroanal. Chem. *763*, 104–109. https://doi.org/10.1016/j.jelechem.2015.12.043.

20. Chen, X., Gross, A.J., Giroud, F., Holzinger, M., and Cosnier, S. (2018). Comparison of Commercial and Lab-made MWCNT Buckypaper: Physicochemical Properties and Bioelectrocatalytic O2 Reduction. Electroanalysis *30*, 1511–1520. https://doi.org/10.1002/elan.201800136.

21. Milton, R.D., Giroud, F., Thumser, A.E., Minteer, S.D., and Slade, R.C.T. (2013). Hydrogen peroxide produced by glucose oxidase affects the performance of laccase cathodes in glucose/oxygen fuel cells: FAD-dependent glucose dehydrogenase as a replacement. Phys. Chem. Chem. Phys. *15*, 19371–19379. https://doi.org/10.1039/C3CP53351D.

22. Kondaveeti, S., Moon, J.M., and Min, B. (2017). Optimum spacing between electrodes in an air-cathode single chamber microbial fuel cell with a low-cost polypropylene separator. Bioprocess Biosyst. Eng. *40*, 1851–1858. https://doi.org/10.1007/s00449-017-1838-3.

23. Cinquin, P., Gondran, C., Giroud, F., Mazabrard, S., Pellissier, A., Boucher, F., Alcaraz, J.-P., Gorgy, K., Lenouvel, F., Mathé, S., et al. (2010). A Glucose BioFuel Cell Implanted in Rats. PLoS One *5*, e10476. https://doi.org/10.1371/journal.pone.0010476.

24. El Ichi, S., Zebda, A., Alcaraz, J.-P., Boucher, F., Boutonnat, J., Cinquin, P., and Martin, D.K. (2014). Biocompatible implantable biofuel cell. In 2014 IEEE Conference on Biomedical Engineering and Sciences (IECBES), pp. 51–55. https://doi.org/10.1109/IECBES.2014.7047553.

25. Weidlich, E., Richter, G., Sturm, F.V., Rao, J.R., Thorén, A., and Lagergren, H. (1976). Animal Experiments with Biogalvanic and Biofuel Cells. Biomater. Med. Devices Artif. Organs *4*, 277–306. https://doi.org/10.3109/10731197609118655.